



UNIVERSITY OF LEEDS

This is a repository copy of *High-Speed Indoor Optical Wireless Links Employing Fast Angle and Power Adaptive Computer-Generated Holograms With Imaging Receivers*.

White Rose Research Online URL for this paper:  
<http://eprints.whiterose.ac.uk/105954/>

Version: Accepted Version

---

**Article:**

Alresheedi, MT and Elmirghani, JMH (2016) High-Speed Indoor Optical Wireless Links Employing Fast Angle and Power Adaptive Computer-Generated Holograms With Imaging Receivers. *IEEE Transactions on Communications*, 64 (4). pp. 1699-1710. ISSN 0090-6778

<https://doi.org/10.1109/TCOMM.2016.2519415>

---

© 2016, IEEE. Personal use of this material is permitted. Permission from IEEE must be obtained for all other users, including reprinting/ republishing this material for advertising or promotional purposes, creating new collective works for resale or redistribution to servers or lists, or reuse of any copyrighted components of this work in other works.

**Reuse**

Unless indicated otherwise, fulltext items are protected by copyright with all rights reserved. The copyright exception in section 29 of the Copyright, Designs and Patents Act 1988 allows the making of a single copy solely for the purpose of non-commercial research or private study within the limits of fair dealing. The publisher or other rights-holder may allow further reproduction and re-use of this version - refer to the White Rose Research Online record for this item. Where records identify the publisher as the copyright holder, users can verify any specific terms of use on the publisher's website.

**Takedown**

If you consider content in White Rose Research Online to be in breach of UK law, please notify us by emailing [eprints@whiterose.ac.uk](mailto:eprints@whiterose.ac.uk) including the URL of the record and the reason for the withdrawal request.



[eprints@whiterose.ac.uk](mailto:eprints@whiterose.ac.uk)  
<https://eprints.whiterose.ac.uk/>

# High-Speed Indoor Optical Wireless Links Employing Fast Angle and Power Adaptive Computer-Generated Holograms with Imaging Receivers

Mohammed T. Alreshedi<sup>1</sup> and Jaafar M.H Elmirghani<sup>2</sup> Senior Member, IEEE

<sup>1</sup> Department of Electrical Engineering, King Saud University, Riyadh, Kingdom of Saudi Arabia

<sup>2</sup> School of Electronic and Electrical Engineering, University of Leeds, Leeds LS2 9JT, UK

[malreshedi@ksu.edu.sa](mailto:malreshedi@ksu.edu.sa), [j.m.h.elmirghani@leeds.ac.uk](mailto:j.m.h.elmirghani@leeds.ac.uk)

**Abstract-** In this paper, we introduce an adaptive optical wireless system that employs a finite vocabulary of stored holograms. We propose a fast adaptation approach based on a divide and conquer methodology resulting in a number of adaptation algorithms: fast angle adaptive holograms (FAA-Holograms), fast power adaptive holograms (FPA-Holograms), and fast angle and power adaptive holograms (FAPA-Holograms) and evaluate these in mobile optical wireless (OW) systems in conjugation with imaging reception. The ultimate goal is to improve the signal to noise ratio (SNR), reduce the effect of inter-symbol-interference (ISI), speed up the adaptation process and eliminate the need to calculate the hologram in real-time at each transmitter and receiver location. The system operates at high data rates under the impact of multipath dispersion, background noise and mobility. At a data rate of 2.5 Gb/s, and under eye safety regulations, the proposed FAPA-Holograms offers around 20 dB SNR in the presence of background shot noise, receiver noise, multipath dispersion and mobility. Simulation results show that the proposed system, FAPA-Holograms, can reduce the time required to identify the optimum hologram position from 80 ms in the original beam angle and power adaptive line strip multibeam system (APA-LSMS) to about 13 ms.

**Index Terms-** finite vocabulary of holograms, mobile optical wireless, signal-to-noise ratio, imaging receiver.

## I. INTRODUCTION

Recently optical wireless (OW) local area networks (LANs) have attracted a great deal of attention due to their potential to provide high-speed transmission through low cost hardware and without interfering with radio frequency devices. Over the last three decades the use of the optical spectrum for indoor communications has been widely studied [1]–[4]. Due to the inherent nature of light, free space Infrared (IR) links offer numerous advantages over their radio frequency (RF) counterparts including an abundant unregulated spectrum, freedom from fading [2], [4] and a degree of privacy at the physical layer as optical signals are confined to the room in which they originate (hence, the possibility of frequency reuse). Despite these advantages, OW systems encounter two major impairments. The first is concerned with sensitivity to additive shot noise owing to sunlight or artificial background lighting. The second is the multipath dispersion associated with reflections from walls, ceiling and room surfaces and the non-line-of-sight (non-LOS) transmission of OW signals. In addition to these drawbacks, there is a limit on the maximum permitted optical power radiated from commercial transmitters. This limit is set by strict eye and skin safety regulations [2], [3].

Recently, many researchers have studied and demonstrated the use of visible light (white-light emitting diodes (LEDs)) for indoor communications [5]–[10]. However, the accomplishment of high transmission rates is a demanding task. This is due to the slow response of phosphor, which limits the modulation bandwidth of white LEDs to a few MHz

[6]. There are however, some approaches that have been proposed to improve the modulation bandwidth of white LEDs [7–10]. In [10] researchers proposed a 3-Gb/s single-LED OFDM-Based wireless VLC link using a Gallium Nitride  $\mu$ LED. Here orthogonal frequency division multiplexing is employed as a modulation scheme and pre- and post-equalization techniques, as well as adaptive data loading are applied in order to achieve 3 Gb/s. It is imperative to note here although the state of the art VLC Gb/s system is able to achieve 3 Gb/s, it requires complex signal processing and advanced modulation formats. On the contrary, IR optical communications can provide high transmission rates similar to visible light systems and potentially higher data rates (data rate up to 10 Gb/s employing OOK modulation can be achieved) [12]–[13]. This is due to the wider modulation bandwidth of laser sources used in IR OW instead of white LEDs. IR optical systems can use simple signal processing functionality and simple modulation formats while having a much higher bandwidth available for future usage. IR OW systems have some additional advantages compared to VLC. For example light dimming is not an issue in IR systems and the uplink implementation using IR is convenient as it avoids bright visible light next to the user equipment, next to laptop for example.

OW transmission links can be classified into two basic schemes: direct line-of-sight (DLOS) and non-LOS (diffuse systems). DLOS can improve power efficiency and minimise multipath dispersion. However this class of systems needs to be carefully aligned in order to set up the link. On the other hand, diffuse transmission links allow the system to operate even when barriers are placed between the transmitter and the receiver which may still allow an independent path. Although they offer full mobility and do not require a direct LOS between the transmitter and the receiver, they suffer from multipath dispersion. Another way to combine the advantages of the directed LOS and diffuse configurations and to overcome the disadvantages is to use a multibeam transmitter that produces multiple diffusing spots in different directions in a room. The multiple diffusing spots can be implemented using computer generated holograms (CGHs) with static beam intensities, (as in [3]) or can be produced using a number of transmitters (as in [4]). Previous work in this area has shown that significant SNR improvement over a conventional diffuse system (CDS) can be achieved by employing a uniform multibeam system [3]. However, mobility and shadowing can induce significant SNR degradation in indoor OW systems. Various techniques have recently been proposed to combat the limitations of OW systems, and higher bit rates have been achieved [11]–[16]. OW links offer the opportunity for high-speed communications and the potential to achieve data rates up to 10 Gb/s with full mobility, although these have not been demonstrated to date experimentally [12], [13]. Experimental multi-gigabits OW systems with limited mobility have been

successfully demonstrated in [15]-[19]. Despite the significant progress achieved to date, more research is required to enable the design of OW systems that realize the potential bandwidth and data rates possible in these systems. The research presented in this paper aims to address the OW systems impairments and propose new practical solutions to allow the system to operate at high data rates such as 2.5 Gb/s and 5 Gb/s with full mobility. It more importantly focuses on speeding-up the adaptation process as well as eliminating the need to calculate a real-time hologram at each transmitter and receiver location.

Beam angle and power adaptation has been shown to be an effective technique that can help optimize the distribution of the diffusing spots and the power among the spots in order to maximize the receiver's SNR, regardless of the transmitter's position, the receiver's orientation and the receiver's field of view (FOV). Simulation results have shown that a significant performance improvement can be achieved in a mobile OW system that employs beam angle and beam power adaptation in a line strip multibeam system (APA-LSMS) [12] – [13]. The improvements achieved are however at the cost of complex system design in the power adaptive line strip multibeam system (PA-LSMS), angle adaptive line strip multibeam system (AA-LSMS) and APA-LSMS. The complexity is associated with the computation time required to identify the optimum spot location, as well as the time needed to generate the hologram that generates beams at the optimum powers and angles. To reduce the system complexity, we introduce a adaptive finite hologram vocabulary approach using simulated annealing to generate multibeam spots. The holograms are pre-calculated and stored in the proposed system (each is suited for a given (range of) transmitter and receiver locations) and eliminate the need to calculate holograms real time at each transmitter and receiver location. The concept of finite adaptive computer-generated holograms was first introduced in our recent work [21]. The work in [21] investigated a very limited case of finite pre-stored holograms and studied it in a realistic indoor environment to examine the impact of shadowing. Here we extend the work in [21] by (i) optimizing the number of holograms to be stored in the system, (ii) studying the trade-offs between computation complexity and SNR penalty and comparing the results to a range of adaptive finite hologram systems, (iii) examining the impact of having a finite hologram vocabulary on SNR and delay spread and comparing the system with the original beam angle and power adaptive system proposed in [12] and (iv) employing high-speed imaging receiver with narrow FOVs.

In this paper we propose and model fast angle adaptive holograms (FAA-Holograms), fast power adaptive holograms (FPA-Holograms), and fast angle and power adaptive holograms (FAPA-Holograms) mobile OW systems, in conjugation with imaging reception. The ultimate goal of the proposed systems is to eliminate the need to calculate holograms repeatedly, as well as speed up the angle and power adaptation algorithm compared with the original adaptive multibeam systems, proposed previously in [12]-[13]. A further improvement can be achieved by increasing the number of holograms in this system to try to approach the performance of the un-constrained (by finite number of choices) angle and power adaptive systems previously introduced. However, increasing the number of holograms leads to an increase in the computation time required to identify the optimum hologram. We have introduced a fast divide and conquer (D&C) algorithm to select the best beam locations in [20]. Here we develop a divide and conquer algorithm to select the best

hologram from among a finite vocabulary of holograms and study the impact of having a finite hologram vocabulary as well as study the trade-offs between computation complexity and SNR penalty and compare the results to a range of systems.

At 2.5 Gb/s, under eye safety regulations, the proposed FAPA-Holograms offers around 20 dB SNR in the presence of background shot noise, receiver noise, multipath dispersion and mobility. The trade-off between complexity and performance in the proposed systems compared to the original multibeam adaptive systems (PA-LSMS, AA-LSMS and APA-LSMS) is of interest and is investigated. At the worst communication path considered, and where the ceiling is divided into 80 regions (6400 holograms are pre-calculated and stored in the system), the proposed FAPA-Holograms system can reduce the time required to identify the optimum hologram position from 80 ms associated with the APA-LSMS configuration [12] to about 13 ms. The FAPA-Holograms system also eliminates the time needed to generate the hologram, which is about 320 ms, at the cost of an SNR penalty less than 1 dB at every transmitter and receiver location in this case.

The rest of the paper is organized as follows: Section II describes the OW system model. The proposed novel configurations based on beam power and angle adaptive holograms are discussed in Section III. The simulation results of finite adaptive holograms versus the original beam power and angle adaptations are given Section IV. A high-speed mobile indoor OW communication system is introduced in Section V. Finally, conclusions are drawn in Section VI.

## II. OW SYSTEM MODEL AND SIMULATION SET-UP

In OW links, intensity modulation with direct detection (IM/DD) is the simplest modulation format and is as such used widely. The IM/DD channel can be modelled as a baseband linear system in which  $x(t)$  is the input power and  $I(t)$  is the photo current received, which results from the integral of the received optical power over the photo detector surface. An indoor OW channel that uses IM/DD can be fully characterised by the impulse response of the channel as given by

$$I(t) = Rx(t) \otimes h(t) + n_b(t) \quad (1)$$

where  $R$  is the photo-detector responsivity,  $t$  is the absolute time,  $\otimes$  denotes convolution,  $n_b$  is the background noise (BN), which is modelled as AWGN, and  $h(t)$  is the impulse response of the channel.

In order to examine the effects of multipath dispersion on indoor OW systems, a propagation simulator was set up for the case of an empty room with dimensions of 4m (width)  $\times$  8m (length)  $\times$  3m (height). The system model and simulation parameters used in this study are similar to our recent work presented in [21]. All the proposed systems use an upright transmitter with 1 W optical power. Furthermore, the significant SNR improvement of the new proposed systems in Section V is used to reduce the transmit power to 80 mW reducing the power density on the adaptive hologram and helping with eye safety.

A custom design imaging receiver is used to reduce the impact of multipath dispersion. In this work, we employed the imaging receiver design proposed in [12]. It is comprised of a single imaging lens and detector array that is subdivided into 200 pixels. The receiver detector array has a photosensitive area of 2 cm<sup>2</sup> and each pixel has an individual area of 1 mm<sup>2</sup>. The reception zone of each pixel (on the ceiling) is varied as the receiver terminal moves around the room over the CP. The

calculation of the new reception zone associated with each pixel is discussed in detail in [12].

At each pixel the received multipath profile from each spot was computed, based on the area that the pixel observes and the pixel's FOV at each receiver location. Various parameters were derived from the simulated impulse response, such as the delay spread and SNR.

- 1) Delay spread is a good measure of signal pulse spread due to the temporal dispersion of the incoming signal. The delay spread of an impulse response is given by [3]:

$$D = \sqrt{\frac{\sum v_i (t_i - \mu)^2 P_{ri}^2}{\sum v_i P_{ri}^2}} \quad (2)$$

where  $t_i$  is the time delay associated with the received optical power  $P_{ri}$ , and  $\mu$  is the mean delay given by:

$$\mu = \frac{\sum v_i P_{ri}^2 t_i}{\sum v_i P_{ri}^2} \quad (3)$$

- 2) The SNR of the received signal can be calculated by taking into account the powers associated with logic 0 and logic 1 ( $P_{s0}$  and  $P_{s1}$ ) respectively. The SNR is given by [22]:

$$SNR = \left( \frac{R(P_{s1} - P_{s0})}{\sigma_0 + \sigma_1} \right)^2, \quad (4)$$

$$\sigma_0 = \sqrt{\sigma_{pr}^2 + \sigma_{bn}^2 + \sigma_{s0}^2} \text{ and } \sigma_1 = \sqrt{\sigma_{pr}^2 + \sigma_{bn}^2 + \sigma_{s1}^2} \quad (5)$$

where  $\sigma_{pr}^2$  represents the receiver noise which is a function of the design used for the preamplifier;  $\sigma_{bn}^2$  represents the background shot noise component and  $\sigma_{s0}^2$  and  $\sigma_{s1}^2$  represent the shot noise associated with the received signal ( $P_{s0}$  and  $P_{s1}$ ) respectively. The signal-dependent noise ( $\sigma_{st}^2$ ) is very small due to the weak received optical signal, see the experimental results reported in [23]. In this study, we used the PIN-FET transimpedance preamplifier proposed in [24]. The background shot noise calculations can be found in [21]. In the imaging receiver, we considered two schemes: selection combining (SC), i.e. select best pixel and maximum ratio combining (MRC). Calculations of SC and MRC methods can be found in our previous work in [12].

### III. ADAPTIVE HOLOGRAM CONFIGURATIONS

In this section, three adaptive multibeam transmitter configurations are presented and analyzed in order to identify the most suitable geometry for use in indoor OW systems.

#### III.A FAA-Holograms

An angle adaptive OW system has recently been introduced [12]-[13]. Beam angle adaptation (beam steering based on liquid crystal devices) was shown to be an efficient technique that can help identify the optimum distribution of the diffusing spots to provide the strongest path between the diffusing spots and the receiver at every transmitter and receiver location. The adaptive transmitter first produces a single spot to scan the walls and ceiling at approximately 8000 possible locations (associated with a  $2.86^\circ$  beam angle increment [12], [13]) in order to identify the best location, then the transmitter generates a hologram that produces a line strip of diffusing spots at the optimum location. These processes require intensive calculations and time on a digital signal processor (DSP). In order to eliminate the need for computing the holograms at each step an adaptation method is introduced where a finite vocabulary of stored holograms is used. The

floor (or ceiling) is divided into regions i.e., eight regions ( $2\text{ m} \times 2\text{ m}$  per region), see Fig. 1. In each region, the transmitter uses a hologram that generates the optimum diffusing spots if the receiver is present in any one of the regions. These holograms can be pre-calculated so as to target the spots near the receiver (in whichever region the receiver may be) based on our angle adaptation algorithm proposed in [12], [13]. The holograms' pixel information is stored in memory in the transmitter. An adaptation algorithm is used where the transmitter tries the stored holograms either sequentially or in a fast manner using a divide-and-conquer approach explained later in this section. The receiver feeds back SNR information to the transmitter enabling the transmitter to choose the best hologram for the given transmitter and receiver locations.

Computer generated holograms can produce spots with any prescribed amplitude and phase distribution. For the fast angle adaptive holograms (FAA-Holograms), all the spots have the same weight (power), (but different phases). CGH's have many useful properties. Spot distributions can be computed on the basis of diffraction theory and encoded into a hologram. Calculating a CGH means the calculation of its complex transmittance. The transmittance is expressed as

$$H(u, v) = A(v, u) \cdot \exp[j\phi(u, v)], \quad (6)$$

where  $A(u, v)$  is its amplitude distribution,  $\phi(u, v)$  is its phase distribution, and  $(u, v)$  are coordinates in the frequency space. The relative phases of the generated spots are the objects of interest. The hologram is able to modulate only the phase of an incoming wavefront, the transmittance amplitude being equal to unity. The analysis used in [3], [25], [26] was used for the design of the CGHs. The hologram  $H(u, v)$  is considered to be in the frequency domain. The pixels' locations in the hologram are defined by the frequency coordinates  $u$  and  $v$  (two dimension). The observed diffraction pattern  $h(x, y)$  is in the spatial domain (far field in the ceiling). They are related by the continuous Fourier transform:

$$h(x, y) = \iint H(u, v) \exp[-i2\pi(ux + vy)] du dv. \quad (7)$$

The hologram structure is an  $M \times N$  array of rectangular cells, with dimension  $R \times S$ . Each cell represents a complex transmittance value  $H_{kl}$ :  $-M/2 < k < M/2$  and  $-N/2 < l < N/2$ . If the hologram is placed in the frequency plane, the diffraction pattern is given by [25]

$$h(x, y) = RS \text{sinc}(Rx, Sy) \sum_{k=-\frac{M}{2}}^{\frac{M}{2}-1} \sum_{l=-\frac{N}{2}}^{\frac{N}{2}-1} H_{kl} \exp[i2\pi(Rkx + Syl)], \quad (8)$$

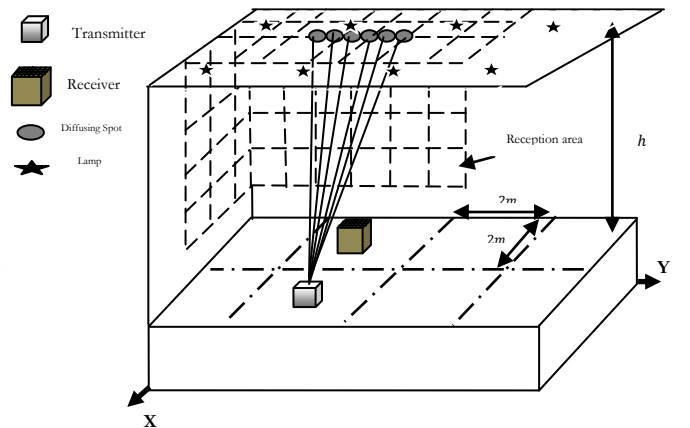


Fig.1: Architecture of our proposed OW system when the transmitter is placed at (3m,3m,1m) and the receiver is at (1m,3m,1m).

where  $\text{sinc}(a, b) = \sin(\pi a) \sin(\pi b) / \pi^2 ab$ . The hologram is designed such that the complex amplitude of the spots is proportional to some value of interest. However, because of the finite resolution of the output device and the complex transmittance of the resulting hologram, the reconstruction will be in error. This error can be used as a cost function. Simulated annealing was employed to minimize the cost function [27]. The amplitudes and phases of every spot are determined by the hologram pixels' pattern and are given by its Fourier transform. The constraints considered in the hologram plane are to discretize the phase from 0 to  $2\pi$  and to achieve a constant unit amplitude for the phase only CGH.

The desired distribution of spots in the far field is  $f(x, y) = |f(x, y)| \exp(i\varphi(x, y))$ . The main goal of the design is to determine the CGH distribution  $g(v, u)$  that generates a reconstruction  $g(x, y)$  as close as possible to the desired distribution  $f(x, y)$ . The cost function (CF) is defined as a mean squared error which can be interpreted as the difference between the normalized desired object energy  $f''(x, y)$  and the scaled reconstruction energy  $g''(x, y)$ :

$$CF_k = \sqrt{\sum_{i=1}^M \sum_{j=1}^N (|f''(i, j)|^2 - |g''_k(i, j)|^2)^2}, \quad (9)$$

where  $f''(x, y)$  represents the normalized desired object energy and  $g''_k(i, j)$  represents the scaled reconstruction energy of the  $k^{\text{th}}$  iteration. Simulated annealing was used to optimize the phase of the holograms offline by minimizing the cost function [27].

For a large room of  $8m \times 4m$ , the floor is divided into eight regions ( $2m \times 2m$  per region). A library which contains 64 holograms optimized offline using simulated annealing was established. Each hologram produces the optimum diffusing spots which were pre-calculated based on an angle adaptation technique [12] in order to optimize the spot locations at each particular area of  $2m \times 2m$ , see Fig. 1. In each region, the transmitter should have eight holograms stored in a library in order to cover the eight possible receiver positions in the room. This results in 64 holograms (in the case of eight regions) that cover the entire room. The total number of holograms required is  $N^2$ , where  $N$  represents the number of regions into which the floor/ceiling is divided. An example of one hologram, when the transmitter is placed at (3m, 3m, 1m) and the receiver is present at the second region, is shown in Fig. 2. Simulated annealing was used to optimize the phase of the computer-generated hologram. Fig. 2 shows three snapshots of hologram phase distributions,  $g(x, y)$ , in the far field at different iterations. When the number of iterations increases, the hologram phase distributions are improved. The cost function versus the number of iterations completed is shown Fig. 3.

After generating  $N$  holograms using simulated annealing optimization, the holograms are stored in the library of the proposed FAA-Holograms system. In the case of classic (i.e. not fast) angle adaptive holograms the transmitter first sequentially tries all  $N$  holograms (64 holograms in this case) and the receiver computes the SNR associated with each hologram at the receiver and relays this information to the transmitter for the transmitter to identify the best hologram to use (update the holograms). This is an exhaustive search mechanism among the stored holograms. If each SNR computation is carried out in  $10 \mu s$  [12], then the total adaptation time when the receiver moves is  $640 \mu s$ . A further improvement in SNR can be achieved by increasing the number of regions on the floor, which leads to smaller regions

and to accurately identifying the receiver's location. A larger number of holograms is generated in this case to choose from leading to an increase in the time required to identify the best hologram. For example, increasing the number of regions from 8 to 16 will lead to an increase in the total number of holograms to 256. Hence the computation time required to identify the optimum holograms is increased to 2.56 ms. In order to overcome this problem a fast angle adaptive hologram (FAA-Holograms) algorithm is introduced to effectively

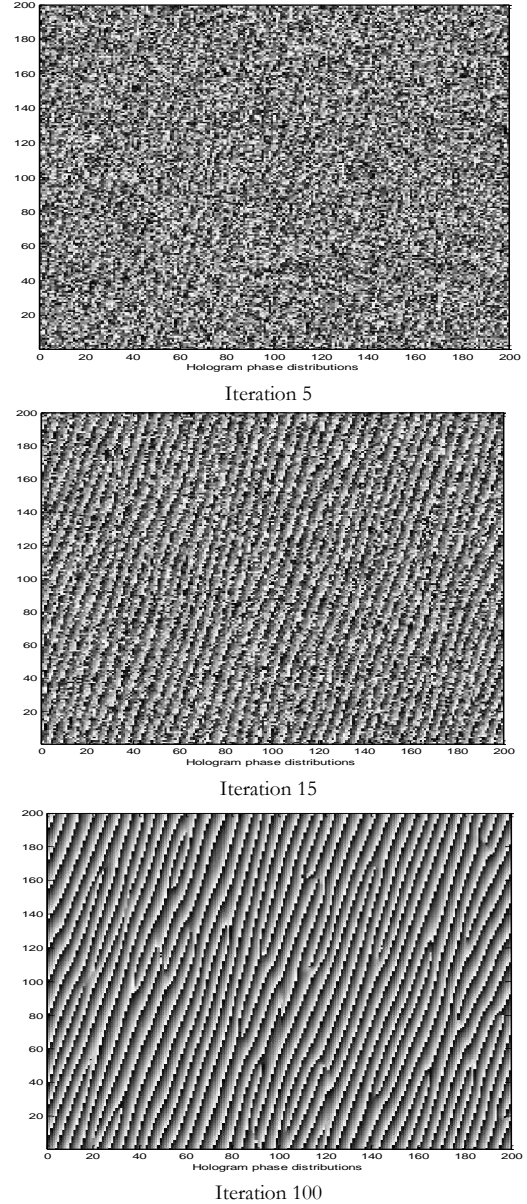


Fig. 2: The hologram phase pattern at Iterations 5, 15 and 100 using simulated annealing optimization. Different gray levels represent different phase levels ranging from 0 (black) to  $2\pi$  (white).

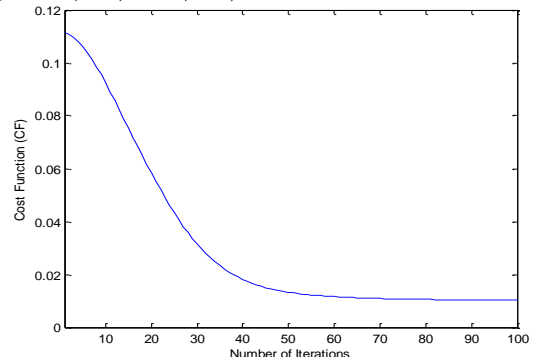


Fig. 3: Cost function versus the number of iterations

improve the SNR (through the use of more holograms) while reducing the computation time required to identify the optimum hologram. The fast algorithm determines the optimum hologram that yields the best receiver SNR based on a D&C algorithm. The transmitter divides the stored holograms into four quadrants with a boundary based on the hologram transmission angles ( $-\delta_{min}$  to 0) and (0 to  $\delta_{max}$ ) in both the  $x$  and  $y$  axes. The transmitter first tries the middle hologram at each quadrant (four holograms will be first tried) to identify the sub-optimal quadrant; hence reducing the number of holograms that need to be tried by a factor of 4 in the first step. The receiver sends a feedback signal at a low rate, which relays to the transmitter the SNR associated with each hologram. The hologram that results in the best receiver SNR is identified as a sub-optimum hologram, and the quadrant that includes this sub-optimum hologram is divided in the next step into four sub-quadrants. The transmitter again scans the middle hologram at four new sub-quadrants and identifies the second sub-optimal hologram; hence identifying the second sub-optimal quadrant. The transmitter again divides the new second sub-optimal quadrant into four quadrants in a similar manner to the first and second sub-optimal quadrants to identify the third sub-optimal quadrant. The quadrant that is represented by the third sub-optimal hologram is then scanned. This technique helps to reduce the computation time required to identify the optimum hologram when a very large number of holograms is used. The proposed FAA-Holograms algorithm can be described for a single transmitter and receiver as follows:

- 1- The transmitter first divides the stored holograms into four main groups associated with four quadrants based on the hologram transmission angles. The boundary angles associated with the first quadrant are  $\delta_{max-x}$  to 0 in the  $x$ -axis and  $\delta_{max-y}$  to 0 in  $y$ -axis.
- 2- The transmitter transmits using the middle hologram in each quadrant in order to determine the first sub-optimum hologram.
- 3- The receiver computes the SNR associated with each transmission (each hologram) and sends a control feedback signal at a low rate to inform the transmitter of the SNR associated with the hologram (four holograms will be tried first in order to find the first sub-optimal hologram / region).
- 4- The transmitter records (the transmission angles of) the hologram where the receiver SNR is sub-optimal. If the transmitter receives more than one equally optimal SNR due to the room symmetry, or due to both the transmitter and receiver being co-located (receiver on the boundary of the optimum region), then the transmitter will select the first hologram from among the available equally good hologram choices and discard the others.
- 5- The transmitter identifies the quadrant that includes the sub-optimal hologram from the hologram's transmission angles, for the next iteration.
- 6- The transmitter again divides the sub-optimal quadrant into four sub-quadrants and repeats steps 3 to 5 to identify the second sub-optimal quadrant.
- 7- The transmitter again divides the second sub-optimal quadrant into four sub-quadrants and repeats steps 3 to 5 to identify the third sub-optimal quadrant.
- 8- The D&C process continues and the transmitter determines the optimal hologram transmission angles that maximize the receiver's SNR.

The proposed system, FAA-Holograms (with 256 holograms), reduces the computation time from 2.56 ms taken by the classic angle adaptive holograms to 160  $\mu$ s. It should be noted that our proposed system operates in an empty rectangular room. In this work, we do not consider the potential interference due to daylight through windows and we do not consider the impact of shadowing in a realistic indoor environment. In the case of a realistic indoor environment, the number of holograms to be scanned in each area should be increased. This will lead to increase in the adaptation process. We have recently studied the impact of shadowing in a realistic indoor environment in [21]. The interference of daylight through windows is of interest and will be considered in future work.

### III.B FPA-Holograms

Beam power adaptation was introduced in [12], [29] with a line strip multibeam OW system (LSMS) to increase the power levels to the spots that are close to the receiver in order to optimize the SNR. The adaptive LSMS switches ON each spot individually and computes the SNR due to this spot at the receiver. The receiver then sends a control feedback signal at a low rate to inform the transmitter of the SNR associated with the beam (spot). The transmitter receives all the SNR weights associated with each spot (80 spots in our case). The transmitter then redistributes the transmit power ( $P_s$ ) among the beams according to the ratio of the SNRs:

$$\text{new power of the spot} = \left( \frac{\text{SNR of the spot}}{\text{Total SNR of the spots}} \right) \times P_s, \quad (10)$$

and then generates a hologram that produces spots with different intensities using a liquid crystal device. These steps require time and calculations to generate the hologram, which increases the transmitter complexity. The idea of beam power adaptation with the finite vocabulary holograms (FPA-Holograms) is to pre-compute holograms (ready to be uploaded to the liquid crystal device) where each hologram represents the best power distribution among the spots using (10) for a given transmitter and receiver location. The floor is divided into regions similar to the FAA-Holograms. Instead of generating  $N^2$  holograms that represent different beam angles as in FAA-Holograms, here the spots are generated vertically above the transmitter, but the power is distributed among the spots to maximize the SNR for the given transmitter and receiver locations. This setting represents one of the  $N^2$  holograms generated and stored. The phase optimization of holograms can be performed in a similar fashion to FAA-Holograms using simulated annealing but with different spot intensities obtained from (10). A fast power adaptive holograms (FPA-Holograms) algorithm is introduced to reduce the time needed to find the best hologram. The fast algorithm is also based on a D&C algorithm that determines the optimum hologram that yields the best receiver SNR. Since the spots' angles in all holograms are equal, the algorithm divides holograms into two main groups based on the power distribution of spots (in the current case LSMS contains 80 spots). The holograms that increase the power level of spot 1 to spot 40 are listed in the first group and the second group represents holograms that increase the power level of spot 41 to spot 80. The transmitter first tries one hologram in each group. The receiver computes the SNR and informs the transmitter about the SNR weight associated with each hologram via a feedback signal. The transmitter determines the sub-optimal hologram that yields the best receiver SNR and the group that includes the sub-optimal hologram is divided into two sub-groups, whereby each sub-group contains the holograms that increase the power level of 20 spots. The

transmitter and receiver continue until the sub-group contains the holograms that increase the power level of five spots. This helps the transmitter to reduce the computation time required to identify the optimum holograms by a factor of 16.

### III.C FAPA-Holograms

Although the FPA-Holograms system is better than LSMS, the fast angle adaptive hologram (FAA-Holograms) system still performs better. This is due the fact that the distance between the diffusing spots and the receiver is a key factor in mobile indoor multibeam OW systems. The benefits of both systems are combined by introducing fast beam angle and power adaptation with a finite vocabulary of holograms (FAPA-Holograms), in order to further improve the system performance under the impact of background noise, receiver noise, multipath dispersion and mobility. The proposed FAPA-Holograms algorithm is similar to the fast angle adaptive algorithm explained above in the way that the optimum hologram is identified. The angles and power levels associated with the spots in each hologram are pre-calculated and stored in the library of the proposed system without adding any complexity at the transmitter when reproducing holograms. It should be noted that the two adaptation algorithms described (angle adaptation algorithm and power adaptation algorithm) apply to a single transmitter and a single receiver position. If there is more than a single transmitter in the room, then a medium access control (MAC) protocol should be used. This will regulate which transmitter-receiver pair can use which resources (for example time slots, code, wavelength) and when. Potential MAC protocols in this environment include carrier sense multiple access (CSMA) [30], packet reservation multiple access [31] and multi-carrier code division multiple access [32] among others. Furthermore opportunistic scheduling [33] can be employed where the optimum hologram is chosen to maximize the SNR in a given region (set of users) for a given time period. The multi-user system can alternatively select the hologram that optimises a given performance criterion. For example it can select the hologram that maximises the minimum SNR among the users, or maximises the sum rate achieved by the users or some other criteria. Moreover, the D&C algorithm needs to be modified in order to speed up the adaptation process in multi-user scenario.

Furthermore, a significant reduction in computation time is observed in the proposed FAPA-Holograms, based on a D&C search algorithm, when the total number of holograms is increased to 6400 (by dividing the floor into 80 regions). The increase in the number of holograms enhances the system SNR (reducing the SNR penalty associated with the use of a finite number of holograms, investigated in Section V). The computation time required to identify the optimum holograms is about 13 ms instead of the 64 ms taken by the classic angle adaptive holograms, as shown in Section V.

## IV. SIMULATION RESULTS OF FINITE ADAPTIVE HOLOGRAMS VERSUS ORIGINAL BEAM POWER AND ANGLE ADAPTATIONS

Simulation results have shown that the beam angle and power adaptations, coupled with imaging receiver detection, can significantly improve performance in a multibeam optical wireless system [12]-[13]. However this is at the cost of complexity in the design of PA-LSMS, AA-LSMS and APA-LSMS. The complexity is associated with the computation time required to identify the optimum spot location, in addition to the time needed to generate the hologram with optimum spot powers and angles. For example, in a typical room with

dimensions of 4 m × 8 m × 3 m (width × length × height), the APA-LSMS system generates a single spot which scans the walls and ceiling by changing the beam angle associated with the spot between  $-90^\circ$  and  $90^\circ$  in steps of  $2.86^\circ$ , a total of 8000 possible locations, which requires 80 ms adaptation time in order to identify the optimum location. The time required to generate the hologram with optimum spot angles and powers can be estimated. If the APA-LSMS system uses the output plane phase optimization (OPPO) algorithm proposed in [34], then the total computation is [34]

$$t_{oppo} = 5 \times p \times S^2 + S \times M \times N, \quad (12)$$

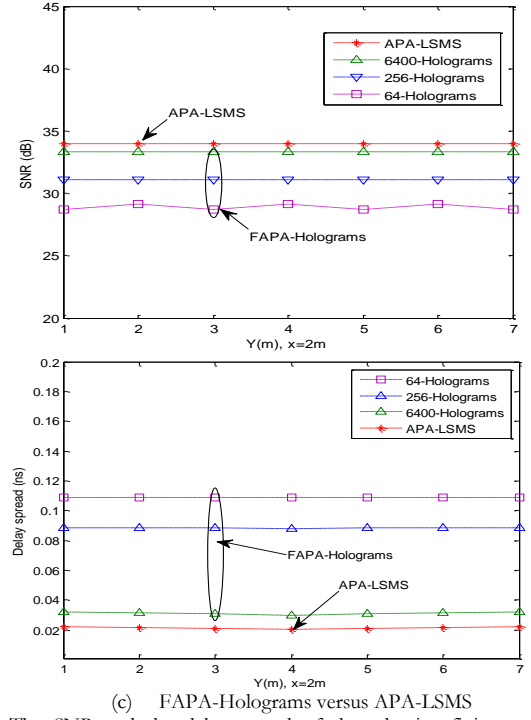
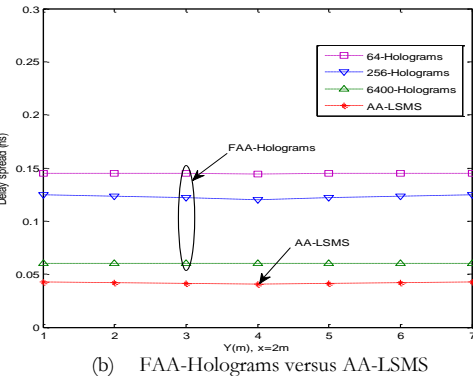
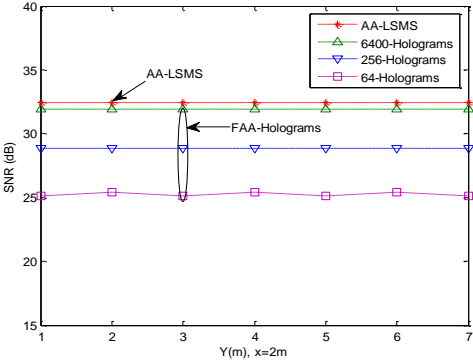
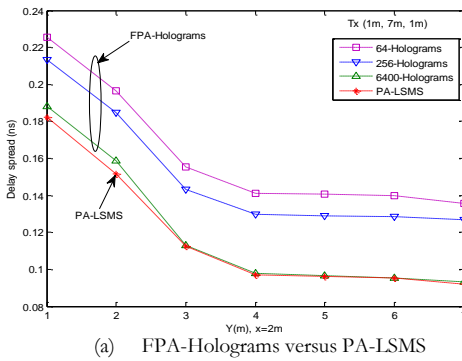
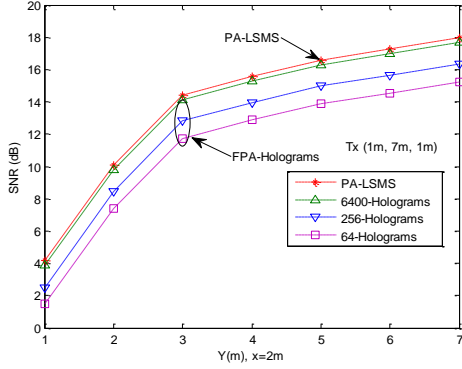
where  $M \times N$  is the number of hologram pixels,  $S$  is the number of spots on the output plane (ceiling),  $p$  is the phase level. The first term ( $5 \times p \times S^2$ , complex operations) represent the computations needed for designing the temporary hologram using direct binary search (DBS) and the second term ( $S \times M \times N$ , complex operations) represents the computation of the hologram using discrete Fourier transform (DFT). If  $M = N = 200$ ,  $S=80$  and  $p=8$ , then:

$$t_{oppo} = 0.2 \times 10^6 + 3.2 \times 10^6$$

The computation for designing the temporary hologram can be ignored based on the study in [34]. If each operation in the optimization of the hologram is carried out in  $0.1\mu s$  then the total time required to generate a hologram is 320ms.

Adaptation based on a finite number of pre-calculated and stored holograms can reduce the computational burden and computation time as previously shown. It is however of interest to establish the penalty associated with the use of different finite vocabularies of holograms. The SNR and delay spread distributions of the fast finite adaptive holograms systems (FPA-Holograms, FAA-Holograms and FAPA-Holograms) are examined when the floor is divided into 8, 16 and 80 regions, see Fig. 4 (a) and (b), (c). All the proposed systems operate at high data rate of 5 Gb/s. The preamplifier used in the 5 Gb/s OW system is the PIN-FET receiver design proposed in [24]. A reduction in the total transmit power under eye safety regulations at high data rates of 1.25 Gb/s, 2.5 Gb/s and 5 Gb/s will be considered in the next section. The SNR penalties of the proposed systems compared with the original PA-LSMS, AA-LSMS and APA-LSMS configurations are shown in Fig. 4. Improvements in the SNR and delay spread are observed in the proposed systems when the total number of regions increases. Increasing the number of regions helps the transmitter produce a hologram that more accurately matches each receiver's location, hence improving the system performance for the given transmitter and receiver locations. Variations (relatively small) in the SNR and delay spread might be present when a small number of holograms, for example, 64 and 256 holograms, are used. This is due to the large size of regions ( $2m \times 2m$  and  $2m \times 1m$ ). Therefore, the SNR and the delay spread results of FAA-Holograms and FAPA-Holograms (with 64 and 256 holograms) in Fig. 4 (b) and (c) have been averaged when the transmitter moves in steps of 1m over the entire room while the receiver moves along the constant line  $x=2m$ . The improvements in the SNR and delay spread are achieved at the cost of computation time required to identify the optimum hologram due to the increase in the total number of holograms. However, the proposed systems use a D&C search algorithm which can help find the optimum hologram with lower computational time compared with classic finite adaptive holograms systems. Furthermore, we increase the number of

holograms that need to be scanned at each quarter to 100 holograms in our fast search algorithm when the proposed system uses a large number of holograms (6400 stored holograms). This can significantly help the transmitter to identify the receiver location. The SNR penalty of the proposed systems compared with the original adaptive OW systems (PA-LSMS, angle adaptive LSMS, and APA-LSMS) is reduced as the number of regions increases, see Fig. 4. At the worst communication link, where the floor is divided into 80 regions (6400 holograms used), a significant computational saving is achieved in the proposed imaging FAPA-Holograms system. Here only 1300 holograms need to be scanned to identify the optimum hologram based on a D&C search algorithm (computation time reduction from 80 ms required for APA-LSMS to 13 ms), can be achieved at the cost of an



(c) FAPA-Holograms versus APA-LSMS  
 Fig. 4: The SNR and the delay spread of the adaptive finite vocabulary holograms (FAPA-Holograms, FAA-Holograms and FAPA-Holograms) versus room location for the original beam power and angle adaptive systems (PA-LSMS, AA-LSMS and APA-LSMS) when the transmitters operate at 5 Gb/s.

SNR penalty of less than 1 dB compared with an APA-LSMS system at each receiver location, see Fig. 4. In addition, the proposed system eliminates the need to generate the hologram (320 ms) when the optimum location is found. All the holograms are pre-calculated and stored in the system, which can further simplify the design of the OW system. Fig. 4 shows the tradeoff between hologram vocabulary size the SNR and delay spread penalties incurred. For a given acceptable SNR (and/or delay spread) penalty, the hologram vocabulary size that should be used can be established.

One of the aims of this paper is to evaluate the efficiency of the fast adaptive algorithm through the study of time complexity. The computational complexity can be calculated based on the nature of the function  $T(n)$  [35], where for example a linear algorithm of input size  $n$  can induce a linear time complexity of  $T(n) = O(n)$ . Usually an algorithm with complexity order  $O(n)$  has a single pass implementation and shows acceptable performance with small  $n$ , however it becomes too complex with larger  $n$ . The classical adaptation algorithm (not fast) can identify the optimum hologram through scanning all the stored holograms, which are processed in the basic “one-pass” style. Therefore, the time complexity of this algorithm is linear given by  $T(n) = O(n)$  and its complexity rises with increase in  $n$ . The input size  $n$  here represents the total number of stored holograms in the proposed system that need to be scanned to identify the optimum hologram that yields in the best SNR. In contrast, the fast algorithm is a recursive algorithm based on a D&C approach, where the scanning process is recursively broken down into a number of iterations  $k$ . Four iterations are conducted in our case (i.e.,  $k = 4$ ), where 4 holograms have to be scanned in each iteration, resulting in a time complexity given as [35]

$$T(n) = j \log_2 \left( \frac{n}{j} \right), \quad (13)$$

where  $j$  is the number of sub-problems (quadrants in our case). In each iteration the fast algorithm divides the scanning area into four quadrants ( $j = 4$ ). Therefore the fast algorithm can achieve time optimal  $O(4 \log_2(n/4))$  complexity, and therefore it is highly efficient compared to the classical algorithm. For example with  $n=6400$ , 256 and 64 holograms;  $k=4$  and  $j=4$ , the reduction in complexity as a result of using the fast D&C algorithm is by factors of 42, 24 and 16 respectively.

Furthermore, the system may choose to update its holograms less frequently even in the presence of mobility. This simplification is at the cost of an SNR penalty. Fig. 5 shows the SNR penalty based on the transmitter using its old hologram settings while in motion. The system design should allow a link margin. For example with a link power margin of 3 dB, the results in Fig. 5 show that adaptation has to be done every time the receiver moves by 1.3 m approximately. We suggest that the receiver periodically (for example at 0.1 second intervals, given a typical pedestrian speed of 1 m/s) re-evaluates its SNR and if this has changed significantly (compared to a threshold value) then this change initiates transmitter adaptation. Therefore the 13 ms adaptation time represents an overhead of 13% in terms of transmission time. It should be noted that this adaptation has been done at the rate at which the environment changes for example the rate at which humans move not at the system's bit rate. Therefore, when the system is stationary it can achieve 5 Gb/s. When it is on the move it can achieve 87% of this data rate, i.e. 4.35 Gb/s. Note that when a small number of detectors is used at the receiver such as three or seven detectors, instead of 200 detectors then the number of hologram to be scanned at each quadrant has to be increased.

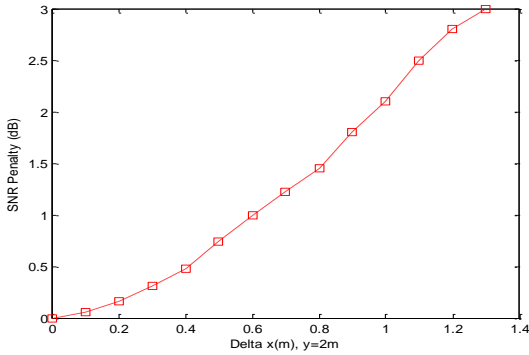


Fig.5. The SNR Penalty of our proposed system when the receiver moves from the optimum location of the spots at (1m, 2m, 1m) along x axis.

Furthermore, we have also examined the impact of designing a finite number of holograms based on a particular room size, and subsequently using the OW system in rooms with different sizes. The holograms were designed for our room with dimensions (4m × 8m × 3m) and the system was then evaluated in two empty rooms (without furnishings) with dimensions of (3m × 6m × 3m) and (5m × 10m × 3m) (width × length × height). The proposed FAPA-Holograms system is compared with the original beam power and angle adaptation (APA-LSMS) system. The latter fully adapts to any room of any size. Fig. 6 shows the results of the proposed system when the transmitter is placed at three different locations: room's centre, room's edge and room's corner while the receiver moves along the  $x=0.5$  m and 1.5 m lines for the room set-up (3m × 6m × 3m) and the  $x=1$ m and 2.5m lines for the room set-up (5m × 10m × 3m). Fig. 6 (a) shows that in the case of a small room configuration, the FAPA- Holograms

system still has an SNR penalty of less than 1 dB compared with the APA-LSMS configuration. This is because with a small room size the FAPA-Holograms system, with 6400 stored holograms, is able to cover the entire room at each transmitter and receiver location (the choices available within the finite vocabulary are still good). However, with a large room size, when the transmitter is near the room edge and the room corner at (2.5 m, 9m, 1m), (1m, 1m, 1m), respectively, and the receiver is placed at the room corner and the room edge at (1m, 1m, 1m), (2.5m, 9m, 1m), respectively, there is a differential SNR penalty of 2.8 dB. In order to reduce the SNR penalty, as well as reduce the effect of the room configuration, finite adaptive holograms system (FAPA-Holograms) can be designed for a large room of (5m × 10m × 3m), where the floor is divided into 100 regions for example. In this case, 10,000 holograms need to be stored in the system memory. A D&C search algorithm can be used to reduce the time required to identify the optimum hologram from 100 ms to around 14 ms.

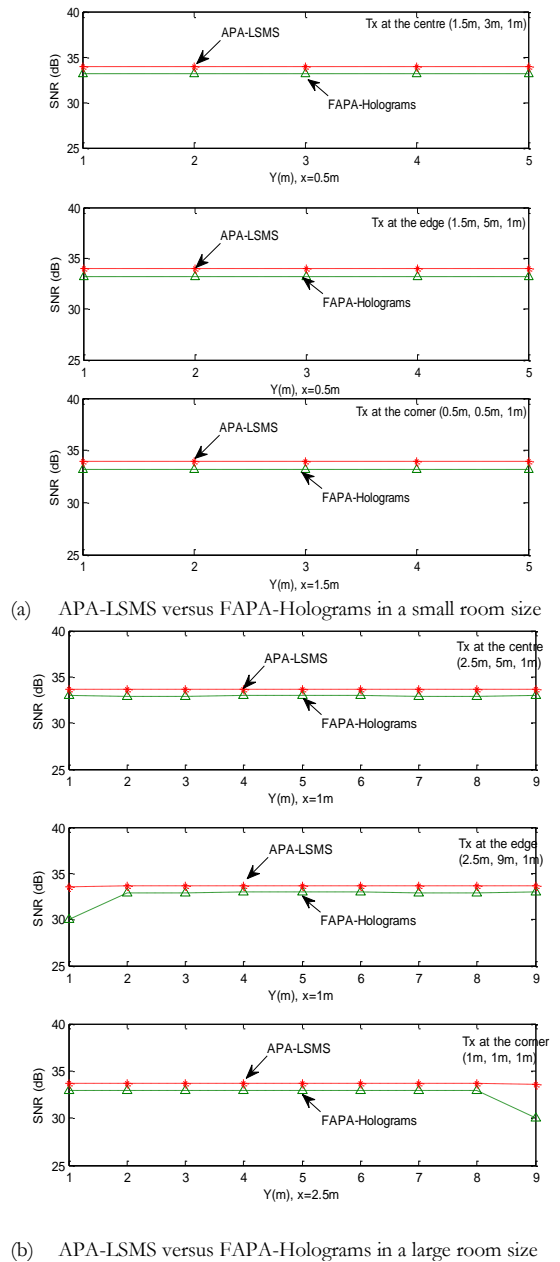


Fig. 6: The SNR of APA-LSMS; and of FAPA-Holograms designed for (4m × 8m × 3m) room but used on rooms of dimensions (a) (3m × 6m × 3m) and (b) (5m × 10m × 3m).

## V. HIGH-SPEED MOBILE INDOOR OW COMMUNICATION SYSTEM

In conventional OOK systems, the SNR has to be 15.6 dB in order to achieve a BER of  $10^{-9}$ . The improvement in the SNR obtained as a result of our new system (FAPA-Holograms) can help the system reduce the total transmit power, while operating at higher data rates of 1.25 Gb/s, 2.5 Gb/s and 5 Gb/s. To further increase the link budget at higher data rates, the number of holograms was increased to 6400 (which reduces the penalty due to the finite number of holograms) by dividing the floor into 80 regions. Note that a relatively small memory size is needed to store  $6400 \times (200 \times 200)$  complex numbers, where each complex number represents the phase of a pixel. At high data rates, we used as preamplifier the PIN-FET receiver design in [24]. In an optical direct detection system, the optimum receiver bandwidth is 0.7 times the bit rate. This means that a 5 Gbit/s data rate requires a 3.5 GHz receiver bandwidth (the 0.7 figure is based on Personik's optical receiver design [36]). Therefore, the bandwidth was limited to 0.875 GHz, 1.75 GHz and 3.5 GHz for the 1.25 Gb/s, 2.5 Gb/s and 5 Gb/s systems, respectively via the use of appropriate filters. The fast algorithm based on D&C only needs to scan/try 1300 holograms to identify the optimum hologram, which significantly reduces the computation time to 13 ms compared with the 64 ms needed in the case of classic angle and power adaptive hologram. To investigate the proposed system, FAPA-Holograms, with respect to eye safety regulations, we used a total transmit power of 80 mW (1 mW per beam). This limitation was introduced in our power adaptation which was not allowed to increase the power per spot beyond 0.5 mW. Again, all the holograms are pre-calculated and stored in the proposed system to eliminate the need to calculate a hologram at each step. The SNRs achieved in the proposed system in this case were about 29 dB, 20 dB and 11 dB at 1.25 Gb/s, 2.5 Gb/s and 5 Gb/s respectively, under the impact of background noise, multipath dispersion and mobility, see Fig. 7. The drop in the SNR is attributed to the reduction in the total transmit power from 1 W to 80 mW, and also due to the power restriction per beam in our algorithm. At 1.25 Gb/s and 2.5 Gb/s the SNR is still greater than 15.6 dB (BER  $< 10^{-9}$ ). Since the FAPA-Holograms system is able to identify the optimum hologram as determined by the receiver, it is possible to use the modified imaging receiver proposed in [12] with our system at 5 Gb/s which can provide an SNR gain of round 7 dB. Furthermore, forward error correction (FEC) can be used with the proposed system

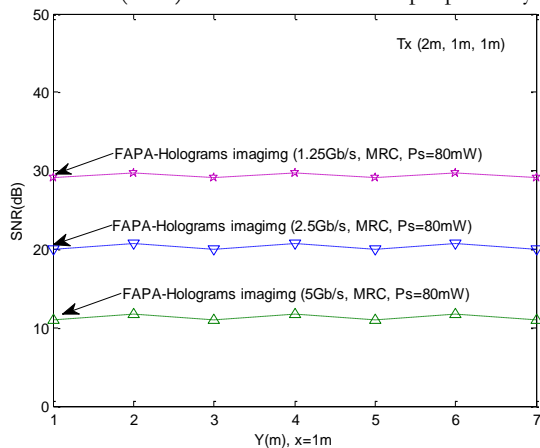


Fig. 7: The SNR of our proposed FAPA-holograms system operating at 1.25 Gb/s, 2.5 Gb/s and 5 Gb/s, with a total transmit power of 80 mW, when the transmitter is placed at (2m, 1m, 1m) and the receiver moves along the x=1m line.

at 5 Gb/s to reduce the BER from  $10^{-3}$  to  $10^{-9}$ . The higher data rates (1.25 Gb/s, 2.5 Gb/s and 5 Gb/s) in the FAPA-Holograms system are therefore feasible through a combination of angle and power adaptive holograms, and imaging receivers. It is worth noting that the hologram system can be modelled analytically, however the signal propagation in the room and the background noise cannot be modelled accurately in closed form analytic expressions, although approximations can be made to the impulse response of certain systems such as the fully diffuse optical wireless system [4]. To the best of our knowledge there are no closed form expressions for the impulse response of adaptive (power, delay and angle adaptation) multi-beam optical wireless systems. The development of such closed form channel impulse response expressions as a function of room size and transmitter and receiver locations is of great interest and will be pursued in future work.

## VI. CONCLUSIONS

Mobility can degrade the performance of the diffuse and spot-diffusing OW systems. In this paper, we introduced adaptive finite vocabulary holograms that are pre-calculated and stored in our proposed system (transmitter) memory. We also introduced a new search algorithm based on D&C in order to reduce the time needed to select the best pre-calculated hologram. Our proposed systems are coupled with an imaging receiver to further improve the received optical signal at the receiver, as well as mitigate the impact of background noise and multipath dispersion. The angle and power associated with the spots in each hologram are pre-calculated and stored in the proposed system without adding any complexity at the transmitter to reproduce (compute) the holograms. The improvements in the SNR and delay spread achieved as a result of the new system (FAPA-Holograms) enables the system to reduce the total transmit power, in addition to operating at high data rates. To investigate the proposed FAPA-Holograms system with respect to eye safety regulations, a total transmit power of 80 mW (1 mW per beam) was used. A limitation was introduced in the power adaptation where the power per spot cannot be increased beyond 0.5 mW. The SNRs achieved in our proposed system in this case were about 29 dB, 20 dB and 11 dB at 1.25 Gb/s, 2.5 Gb/s and 5 Gb/s respectively, under the impact of background noise, multipath dispersion and mobility. The SNR and delay spread results of our proposed systems (FAPA-Holograms, FAA-Holograms and FAPA-Holograms) were examined and compared with the original OW adaptive systems (PA-LSMS, AA-LSMS and APA-LSMS) proposed in our previous work. Improvements in the SNR and the delay spread in the proposed systems were observed and found to be close to original adaptive OW systems, when the total number of holograms stored increases.

Increasing the number of holograms / regions helps the transmitter accurately identify the receiver's location, hence improving the system performance. A search algorithm based on D&C was used in order to reduce the time needed to select the best pre-calculated hologram. In the worst communication path considered, when the floor is divided into 80 regions (6400 holograms are pre-calculated and stored in the system), our proposed system FAPA-Holograms reduces the time required to identify the optimum hologram position from 80ms for the APA-LSMS configuration to about 13 ms, at the cost of an SNR penalty of less than 1 dB at every transmitter and receiver location. In addition, the proposed systems eliminate the need to compute/generate the hologram (320ms) when the optimum location is found. This fast algorithm is

only required to scan 1300 holograms to identify the best hologram based on a D&C algorithm. Moreover, different room sizes were considered to examine the performance of the adaptive finite vocabulary hologram system when it is designed for a given room size and used in rooms with different sizes. The proposed system is less sensitive to room geometry (when the design is made for a large room (5m, 10m, 3m)), which results in an extended range of beam angles that readily accommodates smaller rooms. The system therefore operates in our case with an SNR penalty of less than 1 dB in all rooms equal to or smaller in size than the design room (which can be selected to be large); crucially though our system offers faster adaptation than previous systems. Future work will consider the experimental implementation of our system and its demonstration in rooms of different sizes. It is also of interest to consider sources that produce spatial power distributions other than those associated with holograms.

## REFERENCES

- [1] D. K. Borah, A. C. Boucouvalas, C. C. Davis, S. Hranilovic, and K. Yiannopoulos, "A review of communication-oriented optical wireless systems," *EURASIP J. Wireless Commun. Netw.*, vol. 91, pp. 1–28, Apr. 2012.
- [2] J. M. Kahn and J. R. Barry, "Wireless infrared communications," *Proc. IEEE*, vol. 85, no. 2, pp. 265-298, Feb. 1997.
- [3] S. Jivkova and M. Kavehard, "Multispot diffusing configuration for wireless infrared access," *IEEE Trans. Communications.*, vol. 48, no. 6, pp. 970-978, June 2000.
- [4] J. B. Carruthers and J. M. Kahn, "Angle diversity for nondirected wireless infrared communication," *IEEE Trans. Communications.*, vol. 48, no. 6, pp. 960-969, June 2000.
- [5] T. Komine and M. Nakagawa, "Fundamental analysis for visible-light communication system using LED lights," *IEEE Transactions on Consumer Electronics*, vol. 50, pp. 100-107, 2004.
- [6] H. Le-Minh, D. O'Brien, G. Faulkner, L. Zeng, K. Lee, D. Jung, and Y. Oh, "High-speed visible light communications using multiple-resonant equalization," *IEEE Photonics Technology Letters*, vol. 20, pp. 1243-1245, 2008.
- [7] C. W. Chow, C. H. Yeh, Y. F. Liu and Y. Liu, "Improved modulation speed of the LED visible light communication system integrated to the main electricity network," *Electronics Letters*, vol. 47, pp. 867-868, 2011.
- [8] H. Le-Minh, D. O'Brien, G. Faulkner, L. Zeng, K. Lee, D. Jung, and Y. Oh, "100-Mb/s NRZ Visible light communications using a postequalized white LED," *IEEE Photonics Technology Letters*, vol. 21, pp. 1063-1065, 2009.
- [9] Vucic, C. Kottke, S. Nerreter, K. Langer, and J.W. Walewski et al, "513 Mbit/s visible light communications link based on DMT-modulation of a white LED," *Journal of Lightwave Technology*, vol. 28, pp. 3512, 2010.
- [10] D. Tsonev, C. Hyunhae, S. Rajbhandari, J.J.D McKendry, S. Videv, E. Gu, M. Haji, S. Watson, A. E. Kelly, G. Faulkner, M.D. Dawson, H. Haas. D. O'Brien, "A 3-Gb/s Single-LED OFDM-Based Wireless VLC Link Using a Gallium Nitride  $\mu$  LED," *IEEE Photonics Technology Letters*, vol. 26, pp. 637-640, 2014.
- [11] G. Ntogari, T. Kamalakis, and T. Sphicopoulos, "Analysis of Indoor Multiple-Input Multiple-Output Coherent Optical Wireless Systems" *IEEE Journal of Lightwave Technology*, Vol. 30, no. 3, pp. 317-324, February 2012.
- [12] M. T. Alresheedi and J. M. H. Elmirghani, "10 Gbit/s Indoor Optical Wireless Systems Employing Beam Delay, Angle and Power Adaptation Methods with Imaging Detection," *IEEE Journal of Lightwave Technology*, vol. 30, no. 12, pp. 1843-1856, 2012.
- [13] M. T. Alresheedi and J. M. H. Elmirghani, "Performance Evaluation of 5 Gbit/s and 10 Gbit/s Mobile Optical Wireless Systems Employing Beam Angle and Power Adaptation with Diversity Receivers," *IEEE J. Select. Areas Commun.*, vol. 29, no. 6, pp. 1328-1340, June 2011.
- [14] D. O'Brien, R. Turnbull, H. L. Minh, G. Faulkner, O. Bouchet, P. Porcon, M. El Tabach, E. Gueutier, M. Wolf, L. Grobe and J. Li, "High-Speed Optical Wireless Demonstrators Conclusions and Future Directions," *J. Lightw. Technol.*, Vol. 30, no. 13, pp. 2181-2187, July 2012.
- [15] H. L. Minh, Z. Ghassemlooy, D. O'Brien, G. Faulkner, "Indoor Gigabit optical wireless communications: Challenges and possibilities," in *Transparent Optical Networks (ICTON)*, 2010 12th International Conference on, 2010, pp. 1-6.
- [16] H. L. Minh, D. C. O'Brien, G. Faulkner, O. Bouchet, M. Wolf, L. Grobe, and J. Li, "A 1.25 Gb/s indoor cellular optical wireless communications demonstrator," *Photonics Technology Letters*, IEEE, vol. 22, no. 21, pp. 1598–1600, Nov. 2010.
- [17] K. Wang, A. Nirmalathas, C. Lim, and E. Skafidas, "Indoor gigabit optical wireless communication system for personal area networks," in *IEEE Photonics Society, 2010 23rd Annual Meeting of the*, 2010, pp. 224-225.
- [18] K. Wang, A. Nirmalathas, C. Lim, and E. Skafidas, "High speed duplex optical wireless communication system for indoor personal area networks," *Optics Express*, vol. 18, no. 24, pp. 25199–25216, Nov. 2010.
- [19] J. Fadlullah, and Mohsen Kavehrad, "Indoor High-Bandwidth Optical Wireless Links for Sensor Networks," *Lightwave Technology, Journal of*, vol. 28, pp. 3086-3094, 2010.
- [20] F. E. Alsaadi, M.A. Alhartomi, and J.M.H.Elmirghani, "Fast and Efficient Adaptation Algorithms for Multi-gigabit Wireless Infrared Systems," *IEEE Journal of Lightwave Technology*, vol. 31, no. 23, pp. 3735-3751, 2013.
- [21] M.T. Alresheedi and J. M. H. Elmirghani "Hologram Selection in Realistic Indoor Optical Wireless Systems with Angle Diversity Receivers," *IEEE journal on optical and networking (JOCN)*, vol.7, No.8, p. 797-813, August 2015.
- [22] E. Desurvire, "Erbium-doped Fiber Amplifiers: Principles and applications," A Wiley-Interscience Publication, New York, 1994.
- [23] A. Moreira, R. Valadas, and A. Oliveria Duarte, "Optical interference produced by artificial light," *Wireless Networks*, vol. 3, no. 2, pp. 131-140, May. 1997.
- [24] Leskovar Branko, "Optical Receivers for Wide Band Data Transmission Systems," *IEEE Trans. Nucl. Sci.*, vol. 36, no. 1, pp. 787-793, Feb. 1989.
- [25] X. D. Zhao, J. Li, T. Tao, Q. Long, and X. Wu. "Improved direct binary searchbased algorithm for generating holograms for the application of holographic optical tweezers," *Optical Engineering*, vol. 51, 2012.
- [26] F. A. Ramirez, "Holography - Different Fields of Application," *InTech*, 2011.
- [27] H. J. Yang, J. S. Cho, and Y. H. Won, B, "Reduction of reconstruction errors in kinoform CGHs by modified simulated annealing algorithm" *J. Opt. Soc. Korea*, vol. 13, no. 1, pp. 92–97, Mar. 2009.
- [29] F. E. Alsaadi; M. Nikkar and J. M. H. Elmirghani, "Adaptive mobile optical wireless systems employing a beam clustering method, diversity detection, and relay nodes," *IEEE Trans. Communications.*, vol. 58, No.3, pp. 869–879, 2010.
- [30] Y. H. Feng; C. X. Fen and L. Jian, "An integrated PHY-MAC analytical model for IEEE 802.15.7 VLC network with MPR capability," *Optoelectronics Letters*, , Vol. 10, Issue 5, pp 365-368, September 2014.
- [31] Qazi, B.R. and Elmirghani, J.M.H., "MAC Protocol for multimedia traffic in optical wireless communications," *Journal of Optical Communications*, vol. 29, No. 3, pp. 164-169, 2008.
- [32] Alsaadi, F.E. and Elmirghani, J.M.H., "Adaptive mobile line strip multibeam MC-CDMA optical wireless system employing imaging detection in a real indoor environment," *IEEE Journal on Selected Areas in Communications*, vol. 27, No. 9, pp. 1663-1675, 2009.
- [33] P. Viswanath, D. N. C. Tse, and R. Laroia, "Opportunistic beamforming using dumb antennas," *IEEE Trans. Inf. Theory*, vol. 48, no. 6, pp. 1277-1294, June 2002.
- [34] A. Georgiou, T. D. Wilkinson, N. Collings, and W. A. Crossland, "Algorithm for computing spot-generating holograms," *Journal of Optics: A pure and applied optics*, vol. 10, no. 1, 2008.
- [35] J. Kleinberg and E. Tardos, *Algorithm Design*. Boston, MA, USA: Pearson Education, 2006.
- [36] Personick S.D. "Receiver design for digital fiber optical communication system, Part I and II," *Bell System Technology Journal*, vol. 52, no. 6 July, Aug.1973, pp 843-886.